

# Capacitance Distribution Analysis Using Wire Mesh Sensor 16×16: A Fluid Detection Case Study in an Industry Exhaust Pipe

Linahtadiya Andiani<sup>1\*</sup>, Amaliyah Rohsari Indah Utami<sup>1</sup>

<sup>1</sup> School of Electrical Engineering, Telkom University, Bandung, 40287, Indonesia

\*linahtadiyaa@telkomuniversity.ac.id

Manuscript received October 30, 2021; revised December 10, 2021; accepted December 27, 2021

## Abstract

The Wire Mesh Sensor (WMS) is a tomography-based sensor that generates an image of the free space distribution in multiphase flow. The resulting distribution image can be the capacitance distribution pattern is detected by the electrode, which is dependent on the fluid parameters. Based on the concepts, the system may be an alternative option for the early detection of waterways. The goal of this study is to evaluate the performance of the WMS system in an industrial exhaust pipe. The ability of the system to identify fluids is determined using the capacitance distribution analysis from the WMS measurement. An exhaust pipe is modeled as a cylinder phantom and simulated to visualize the capacitance distribution. The WMS technique is used on a phantom made up of a homogeneous and inhomogeneous medium with changing fluid differences. The capacitance distribution of each fluid in the phantom is different. It is caused by differences in the relative permittivity of each fluid. The performance of the WMS system is evaluated by looking at the capacitance distribution changed as the geometry of the fluid volume varied. Based on the results, the WMS system is shown to be capable of easily distinguishing variations in fluid volume percentage.

*Keywords:* Capacitance distribution; Exhaust pipe; WMS

DOI: 10.25124/jmeecs.v8i2.4268

## 1. Introduction

The significant increase in waste production can be caused by several factors, including rapid population growth, industrial development, urbanization expansion, and consumerism[1]. Industrial waste is one of the causes of increased environmental pollution. The waste comes from various industrial activities, including materials that are not useful during the manufacturing process such as the food and chemical industry, factories, and mining operations. Environmental pollution by the industrial revolution is a major problem facing the

world today. Most of the industrial wastes without proper treatment cause severe health impacts through the air, water, and soil pollution[2]. Various kinds of industrial waste are exploiting aquatic life. Effects of water pollution caused by industry are very harmful to the organism, which may cause severe kinds of diseases[3].

Currently, wastewater is diverted from houses into waterways via gutters and canals, eventually ending up in rivers, streams, lakes, and oceans that people use[4]. Based on waste management, one of the efforts that can be performed to prevent hazardous

waste pollution is through early detection of waterways connected to industrial waste disposal[5]. The goal of waterways detection is to avoid environmental degradation by safely disposing of industrial wastewater created during water consumption[6]. Imaging technology is one of the technologies being researched to monitor water quality[7]. An alternative imaging technology that is intrusive using a wire-mesh system is being developed. This system is capable of detecting the type of fluid or anomaly that flows through it and displaying it as an image[8].

Wire mesh sensor (WMS) is a sensor that is used to obtain an image of the distribution of free space [9] in a multiphase flow[10]. Multiphase refers to a mixture of two or more physically dissimilar fluids[11]. WMS works by measuring the electrical characteristics of the fluid, such as conductivity and permittivity (or dielectric constant). The electrical characteristics can be used to generate the flow's derived parameters[12]. Basically, the principal of the system is sensor-based flow tomography[13]. The system can be described as a hybrid solution between invasive local measurement of phase fraction[14] and tomographic cross-sectional imaging[15]. Moreover, the forward model of measurement using WMS in the form of capacitance distribution, has been proven to be useful in analyzing the fluid height in a pipe and represents electrical characteristics of the fluid in the pipe [16]. This is consistent with the concept of capacitance ( $C$ ), which is directly proportional to relative permittivity ( $k$ ) and is written in Eq.1.

$$C = \frac{k\epsilon_0 A}{d} \tag{1}$$

where  $A$  was wire surface area and  $d$  was distance between electrodes.

The WMS sensor consists of two parts, namely the transmitter and the receiver. The transmitter wire is 90° apart from the receiver wire. The transmitter and receiver are separated axially by a specified amount of space. one of the transmitter's active electrodes is exposed to an electrical signal. This is not delivered directly to the receiver layer due to the distance between the layers in the first measurement. The other transmitter electrodes are linked to the ground and serve as a passive electrode. Each receiver receives the electrical signal, which is analyzed throughout the picture reconstruction process[17].

The WMS system has been successfully implemented in various of detection systems, such as

the detection system for a mixture of oil and water in an offshore oil refinery pipeline[18] and the solar thermal detection system in steam power plants[19]. It is required to assess the condition of the multiphase fluid using capacitance distribution analysis, based on the results of previous studies.

In this study, an analysis of the capacitance distribution for variations in fluid conditions was performed to assess the performance of the wire mesh sensor system. The fluid volume in the geometry of the exhaust pipe phantom was studied at various geometries. The software was used in this study to model and simulate a WMS 16×16 system in an exhaust pipe from the industry. However, the analysis of the detected fluid type and its application are still limited in this early stage of development.

## 2. Methods

### 2.1 Modeling

The modeling stage consists of the the geometric manufactures and the physics parameters determination of geometric designs. In this study, the geometries were the phantom geometry of an exhaust pipe, the WMS geometry, and the fluid volume geometry.

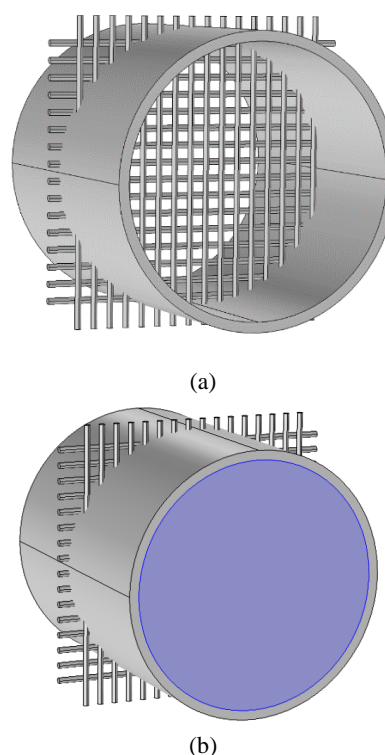


**Figure 1** WMS geometry in-cylinder phantom geometry with (a) air and (b) liquid medium

The manufacture of an exhaust pipe and WMS geometry was shown in Figure 1. A cylinder representing the exhaust pipe has an outer diameter of 14 cm, an inner diameter of 13 cm, and a length of 15 cm. The WMS geometry was designed with 16×16 electrodes. The sensor geometry was formed from two parts, namely the transmitter and the receiver were placed crosswise and separated by a small gap. For each wire was given a diameter of 0.3 cm and a length of 15 cm. Cylindrical phantom geometry models containing air medium and liquid medium are shown in Figure 1a and 1b, respectively.

To assess the performance of the WMS system, the capacitance distribution was measured with varying different fluid materials and volume ratios in the geometry of the exhaust pipe phantom. The single-phase and multiphase conditions were used to analyze the data for this study. In this study, the condition of two types of fluids flowing in separate phases was referred to as a multiphase condition. Several fluid combinations were evaluated in multiphase conditions, such as water-air, water-oil, and oil-air. A volume ratio analysis was also performed for each combination, such as 1:3, 1:1, and 3:1.

**2.2 Simulation**

After obtaining the geometry of the phantom and the system, the simulation stage of geometric design was done by the simulated electrostatics in 3-dimension to obtain the distribution of the phase fraction in the form of capacitance distribution in the exhaust pipe of the industry using the WMS system. The capacitance distribution obtained was used to produce a visualization of the fluid behavior in the industry exhaust pipe.

The simulation parameters are listed in Table 1. The subdomain and boundary of geometry, geometry meshing, and physical solver were chosen to imitate the original condition.

**Table 1** Simulation parameter

Parameter	Set
Dimension	3D
Subdomain	1. Phantom (PVC) 2. WMS (Copper) 3. Fluid (Air; Water; Oil)
Boundary	Terminal 1. Wire 1-16 (Tx 1-16) 2. Wire 17-32 (Rx 1-16)

Geometry Meshing	Normal
Physical Solver	Electronics (Ec)
Physical Study	Stationary
Gridding Voxels	32×32×32 (Scale: mm)
Variation Condition (Fluid Volume Ratio)	1. Water-Air (1:3; 1:1; 3:1) 2. Water-Oil (1:3; 1:1; 3:1) 3. Oil-Air (1:3; 1:1; 3:1)

The setting of the subdomain stage provides the type of material and physical parameters. In this simulation, the cylindrical phantom was PVC pipe and the outside of the phantom was an air chamber. Copper wire was used for the electrodes. The relative permittivity of the materials can be seen in Table 2.

**Table 2** Physical parameter

Material	Relative Permittivity
PVC	2.9
Air	1
Water	80
Oil	4
Copper	1 apakah betul nilainya?

To set the WMS electrode boundary, the stage of boundary setting was performed. At this stage, each wire was defined as a terminal. The injection of voltage through the terminals on the transmitter part (Tx) and the capacitance were measured from the terminals on the receiver part (Rx) as shown in Figure 2. At the measurement process, one of the transmitter terminals acts as a 5 V voltage source and the other of the transmitter terminals act as ground.

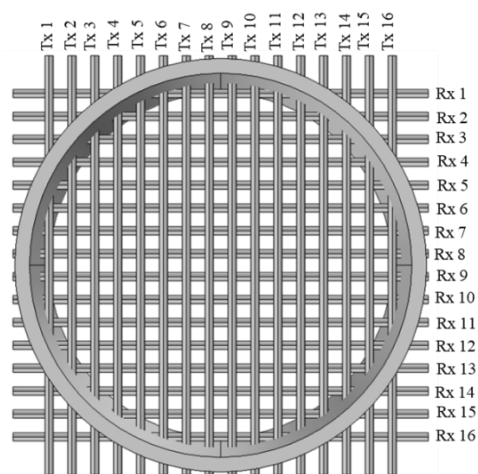


**Figure 2** Boundary setting of WMS system

To obtain accurate data, the setting of the meshing parameter was performed. The measurement of the WMS system with 16x16 electrodes produced 256 data. Every measurement data was the result of normal meshing as shown in Figure 3.

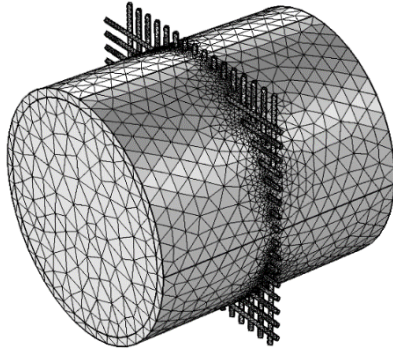


Figure 3 Normal meshing of measurement data

The last simulation stage was to set the physical solvers. In this stage, the parameters were related to the physics concept and physical study method. This study aimed to obtain the capacitance distribution, so the electrostatics was set as a physical solver parameter and the capacitance was analyzed in stationary mode of study method parameter.

The capacitances were obtained by gridding of voxels method in 3-dimensional with 32x32x32 voxels as a cubic volumetric display. The capacitance values of each mesh point at x, y, and z axes were defined as  $C_x$ ,  $C_y$ , and  $C_z$ . The formula used to compute the capacitance ( $C$ ) is presented in Eq. 2.

$$C = \sqrt{C_x^2 + C_y^2 + C_z^2} \tag{2}$$

The data iteration stage was performed to obtain the capacitance from every receiver for each measurement. In this study, the WMS system had 16 transmitter electrodes, so the measurements were repeated 16 times for each transmitter terminal looping.

The data visualization was performed in the last stage to obtain the capacitance distribution of the exhaust pipe geometry. The capacitance data obtained by a receiver terminal was measured at the intersection point between the receiver terminal and the voltage-injected transmitter terminal. At this stage, each capacitance data was put into a 2-dimensional array according to the position of the intersection point..

### 3. Results

#### 3.1. Capacitance Distribution in Homogeneous Medium

The capacitance distribution generated by the WMS system on exhaust pipe geometry is conducted in a homogeneous medium. This study is aimed to obtain the performance of the WMS system for detecting single-phase fluids in simulated pipe. The single-phase fluids used in this study is air, water, and oil. The given fluid volume is 1,990.98 cm<sup>3</sup>.

From the simulation result, the capacitance data were acquired and processed to visualize cross-sectional single-phase fluids. The average capacitance value are 12.8 pF, 735 pF, and 40.4 pF for air, water, and oil, respectively. The largest average capacitance value was got from the measurements on the water fluid while the smallest average capacitance value was got from the measurements on the air-fluid. It was obtained that the capacitance depends on the relative permittivity of the fluid.

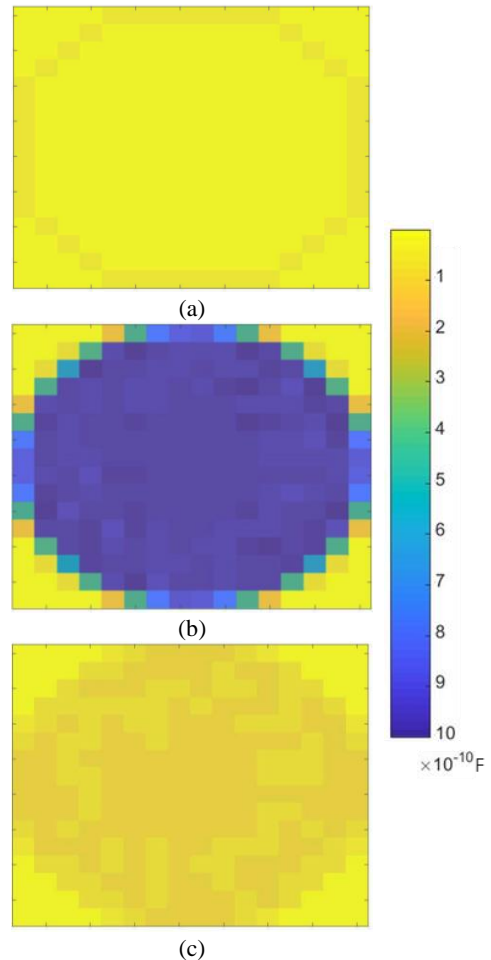


Figure 4 Capacitance distribution in a homogeneous medium for (a) air, (b) water, and (c) oil

Figure 4a depicts the cross-sectional image of the measurement points generated from the WMS system on the air-filled exhaust pipe. The yellow color that has been generated from the image reconstruction shows the capacitance distribution of air-fluid. The darker circle was created using intersection points of the pipe shell. The pipe material has a varied relative permittivity, as was previously recognized. It led to a color gradient in the image.

The cross-sectional image of the capacitance distribution created by the WMS system on the water-filled exhaust pipe is shown in Figure 4b. The color gradient in the capacitance distribution image is more contrast. The capacitance distribution of water-fluid was depicts by the blue pattern created by the image reconstruction. The yellow color on the corner is the result of measuring the capacitance of the crossing point of the pipe on the exterior.

Figure 4c depicts a cross-sectional view of the capacitance distribution formed by the WMS system on an oil-filled exhaust pipe. The result of image reconstruction on oil fluid was nearly identical to the image reconstruction on air fluid. The capacitance distribution of the oil was depicts in dark yellow. The color was nearly identical to the color obtained at the measurement point of the pipe shell.

**3.2 Water and Air Multiphase Detection**

A simulation of the WMS system in pipes filled with water and air was carried out to determine the performance of the WMS system in detecting multiphase fluids in industrial exhaust pipes.

Figure 5 depicts a cross-sectional view of the capacitance distribution for each volume ratio. The color gradient of the image depicts the distinction between two different fluids in the pipe. The capacitance distribution of water fluid is shown in blue, whereas the capacitance distribution of air-fluid is shown in yellow. In this simulation, the color created by image reconstruction is the same as in homogenous medium.

The capacitance distribution of air-fluid is more dominant than that of water-fluid, as shown in Figure 5a. The dominant yellow area in compared to the blue color showed it. It is matched with the fluid volume ratio used in the simulation perfectly. When the fluid volume ratio is 1:1, the yellow and blue patterns in Figure 5b has the same area. When the volume of water exceeds the volume of air (75 % percent of the

volume of pipe), the blue area is more dominant than the yellow area, as shown in Figure 5c.

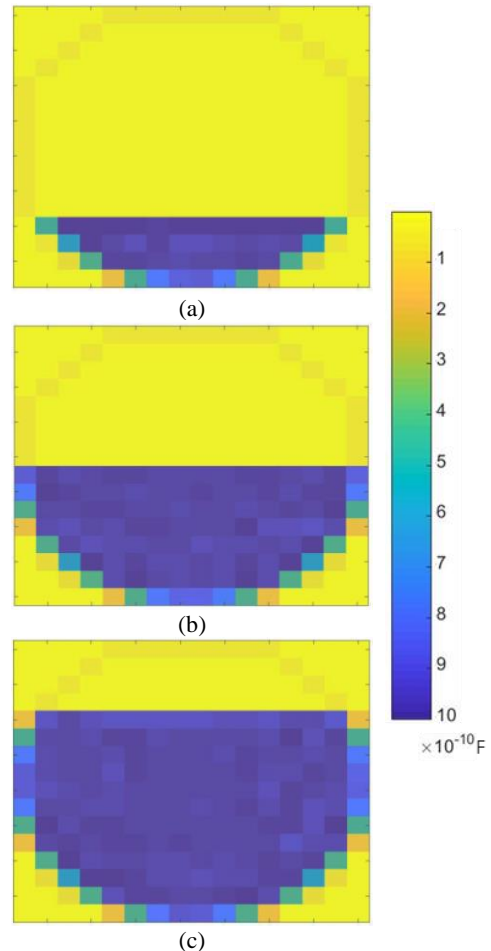


**Figure 5** Capacitance distribution in the multiphase flow of water and air for volume ratio are (a) 1:3, (b) 1:1, and (c) 3:1.

Based on the results, the 16×16 WMS system is shown to be capable of appropriately detecting multiphase liquid in the exhaust pipe and displaying images based on the given volume ratio.

**3.3 Water-Oil and Oil-Air Multiphase Detection**

In addition to study water-air multiphase variations, a study was also aimed at water-oil and oil-air multiphase variations. For each volume ratio of water-oil, Figure 6 shows a cross-sectional view of the capacitance distribution. The color gradient of the image represented the separation of two different fluids in the pipe. Water-fluid capacitance distribution is represented in blue, whereas oil-fluid capacitance distribution is represented in dark yellow. The color obtained by picture reconstruction in this simulation is the same as in the single-phase study.

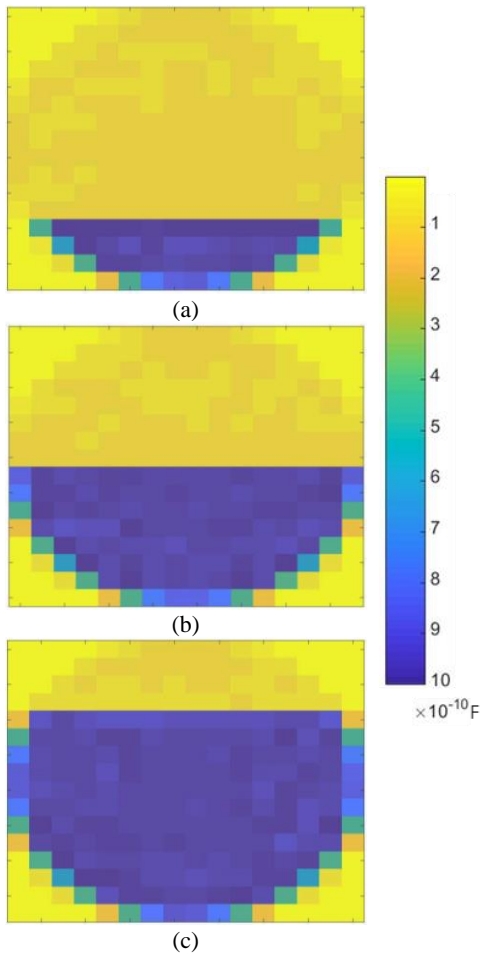


**Figure 6** Capacitance distribution in the multiphase flow of water and oil for volume ratio are (a) 1:3, (b) 1:1, and (c) 3:1

The capacitance distribution measured by the WMS system accurately depicts variations in the water-oil volume ratio. When the volume of oil is more than the volume of water, the resultant capacitance is distributed as shown in Figure 6a. The capacitance distribution is shown in Figure 6b when a comparable volume ratio of oil and water was used. Figure 6c depicts the capacitance distribution that was created when the water volume ratio was greater than the oil volume ratio.

The color gradient in Figure 7 reflects the separation of two separate fluids in the pipe, much like in case of water-air detection. The distribution of air-fluid capacitance is shown in light yellow, whereas the distribution of oil-fluid capacitance as shown in dark yellow. In this simulation, the color acquired by image reconstruction is the same as in the single-phase study.

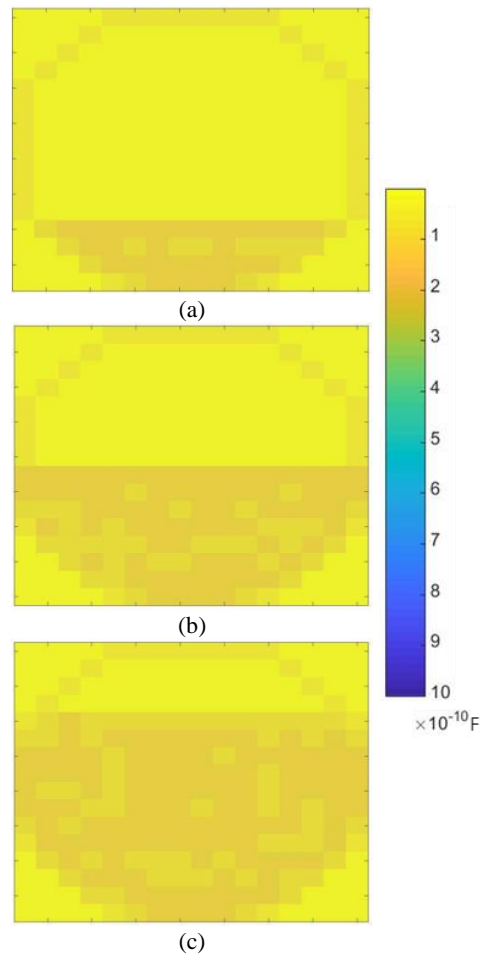


**Figure 7** Capacitance distribution in the multiphase flow of oil and air for volume ratio are (a) 1:3, (b) 1:1, and (c) 3:1

#### 4. Conclusions

In this study, the WMS technique was used on a phantom made up of a homogeneous and inhomogeneous medium with changing fluid differences. The capacitance distribution of each fluid in the phantom was different due to the differences in the relative permittivity of each fluid. The 16×16 WMS system was determined to be capable of correctly detecting single-phase fluid in the exhaust pipe. The relative permittivity of the fluid was found to affect the capacitance distribution imaged by the measurement device. The designed WMS system also could distinguish two fluids with almost identical relative permittivity. Furthermore, the system could appropriately show the capacitance distribution, which depicts the oil-air fluid volume ratio in the pipe. The performance of the WMS system was evaluated by looking at the capacitance distribution changed as the geometry of various fluid volumes. The WMS

system was shown to be capable of easily distinguishing variations in fluid volume percentage. The image quality generated from the capacitance measurement using the WMS 16×16 system was able to show volume ratio variations of single and multiphase fluids. A 16×16 WMS system will be able to detect multiphase fluids in industrial exhaust pipes in the future hardware development of wire mesh sensor systems. To acquire a higher picture resolution, a larger number of meshes might be used in future studies.

### Acknowledgment

This study was supported by the Direktorat Penelitian dan Pengabdian Masyarakat (PPM) Telkom University under the Applied Basic Research Program 2021.

### Reference

- [1] M. Farzadkia, S. Jorfi, M. Nikzad, and S. Nazari, Evaluation of industrial wastes management practices: Case study of the Savojbolagh industrial zone, Iran, *Waste Manag. Res.*, vol. 38, no. 1, pp. 44–58, 2020, doi: 10.1177/0734242X19865777.
- [2] C. G. Awuchi, Industrial Waste Management : Brief Survey And Advice To Cottage , Small And Medium Scale Industries In Uganda Department of Biological and Envi, *Int. J. Adv. Acad. Res. / Sci. Technol. Eng.*, vol. 3, no. 1, pp. 26–30, 2017.
- [3] A. Arif, Water pollution and industries, *Pure Appl. Biol.*, vol. 9, no. 4, 2020, doi: 10.19045/bspab.2020.90237.
- [4] J. N. Edokpayi, J. O. Odiyo, and O. S. Durowoju, Impact of Wastewater on Surface Water Quality in Developing Countries: A Case Study of South Africa, *Water Qual.*, 2017, doi: 10.5772/66561.
- [5] S. N. Zulkifli, H. A. Rahim, and W. J. Lau, Detection of contaminants in water supply: A review on state-of-the-art monitoring technologies and their applications, *Sensors Actuators, B Chem.*, vol. 255, pp. 2657–2689, 2018, doi: 10.1016/j.snb.2017.09.078.
- [6] K. K. Vadde, J. Wang, L. Cao, T. Yuan, A. J. McCarthy, and R. Sekar, Assessment of water quality and identification of pollution risk locations in Tiaoxi River (Taihu Watershed), China, *Water (Switzerland)*, vol. 10, no. 2, 2018, doi: 10.3390/w10020183.
- [7] Z. Wang, B. Li, and L. Li, Research on water quality detection technology based on multispectral remote sensing, *IOP Conf. Ser. Earth Environ. Sci.*, vol. 237, no. 3, 2019, doi: 10.1088/1755-1315/237/3/032087.
- [8] H. M. Prasser, A. Böttger, and J. Zschau, A new electrode-mesh tomograph for gas-liquid flows, *Flow Meas. Instrum.*, vol. 9, no. 2, pp. 111–119, 1998, doi: 10.1016/S0955-5986(98)00015-6.
- [9] R. Kipping, R. Brito, E. Scheicher, and U. Hampel, Developments for the application of the Wire-Mesh Sensor in industries, *Int. J. Multiph. Flow*, vol. 85, no. 2016, pp. 86–95, 2016, doi: 10.1016/j.ijmultiphaseflow.2016.05.017.
- [10] W. Wangjiraniran, Y. Motegi, S. Richter, H. Kikura, M. Aritomi, and K. Yamamoto, Intrusive effect of wire mesh tomography on gas-liquid flow measurement, *J. Nucl. Sci. Technol.*, vol. 40, no. 11, pp. 932–940, 2003, doi: 10.1080/18811248.2003.9715436.
- [11] A. Terenzi, B. Marchetti, M. Leporini, P. Poesio, and J. Liu, Experimental and Numerical Study of Multiphase Flow Phenomena and Models in Oil & Gas Industry, *Petroleum*, vol. 5, no. 2, p. 113, 2019, doi: 10.1016/j.petlm.2019.04.004.
- [12] F. D. A. Dias, P. Wiedemann, M. J. da Silva, E. Schleicher, and U. Hampel, Tuning capacitance wire-mesh sensor gains for measurement of conductive fluids, *Tech. Mess.*, vol. 88, no. S1, pp. S107–S113, 2021, doi: 10.1515/teme-2021-0055.
- [13] M. H. F. Rahiman, L. T. Siow, R. A. Rahim, Z. Zakaria, and V. Ang, Initial study of a wire mesh tomography sensor for Liquid/Gas component Investigation, *J. Electr. Eng. Technol.*, vol. 10, no. 5, pp. 2205–2210, 2015, doi: 10.5370/JEET.2015.10.5.2205.
- [14] A. I. Hameed, L. A. Abdulkareem, and R. A. Mahmood, Experimental Comparison Between Wire Mesh and Electrical Capacitance Tomography Sensors to Predict a Two-Phase Flow Behaviour and Patterns in Inclined Pipe, *Tech. Rom. J. Appl. Sci. Technol.*, vol. 3, no. 5, pp. 49–63, 2021, doi: 10.47577/technium.v3i5.3938.
- [15] F. D. A. Dias et al., New Algorithm to Discriminate Phase Distribution of Gas-Oil-Water Pipe Flow with Dual-Modality Wire-Mesh Sensor, *IEEE Access*, vol. 8, pp. 125163–

125178, 2020, doi:  
10.1109/ACCESS.2020.3007678.

- [16] A. Sujiwa, Wire-Mesh  $16 \times 16$  Capacitance Sensor for Analysis of Capacitance Distribution on Cylindrical Pipe, in *IPTEK Journal of Proceedings Series*, 2018, pp. 130–135, doi: <http://dx.doi.org/10.12962/j23546026.y2018i1.3524>.
- [17] M. J. Da Silva, E. Schleicher, and U. Hampel, Capacitance wire-mesh sensor for fast measurement of phase fraction, *Meas. Sci. Technol.*, vol. 2245, no. 18, 2007, doi: 10.1088/0957-0233/18/7/059.
- [18] I. H. Rodriguez, H. F. V. Peña, A. B. Riaño, R. A. W. M. Henkes, and O. M. H. Rodriguez, Experiments with a Wire-Mesh Sensor for Stratified and Dispersed Oil-Brine Pipe Flow, *Int. J. Multiph. Flow*, vol. 70, no. 2015, pp. 113–125, 2014, doi: 10.1016/j.ijmultiphaseflow.2014.11.011.
- [19] M. Berger, M. Mokhtar, C. Zahler, D. Willert, A. Neuhäuser, and E. Schleicher, Two-phase flow pattern measurements with a wire mesh sensor in a direct steam generating solar thermal collector, in *AIP Conference Proceedings*, 2017, vol. 1850, no. 1, pp. 070003-1–8, doi: 10.1063/1.4984417.



**Amaliyah Rohsari Indah Utami**

was born in Jember, in 1977. She received the Bachelor of Engineering degree in Engineering Physics Department, Sepuluh Nopember Institute of Technology (ITS) Surabaya in 2000 and received the Master of Science degree in Physics Department, Sepuluh Nopember Institute of Technology (ITS) Surabaya in 2010. She is currently a Lecturer in the Engineering Physics Department, School of Electrical Engineering, Telkom University. Her research focuses are on biomass, bio-renewable energy, instrumentation, and biomaterial.



**Linahtadiya Andiani** was born in Semarang, in 1994. She received the Bachelor of Science degree in Physics Department, Sepuluh Nopember Institute of Technology (ITS) Surabaya in 2017 and received the Master of Science degree in Physics Department, Sepuluh Nopember Institute of Technology (ITS) Surabaya in 2019. She is currently a Lecturer in the Engineering Physics Department, School of Electrical Engineering, Telkom University. Her research focuses are on instrumentation, computational physics, and medical physics.